Simulation-based accuracy investigation of a photogrammetric setup to measure a dynamic process

Simon Nietiedt*[1], Thomas Luhmann[1]

[1]Jade University of Applied Sciences, Ofener Str. 16/19, 26129 Oldenburg, Germany

Technical Commission II

KEY WORDS: Close-Range Photogrammetry, Dynamic, Monte Carlo simulation, Kernel density estimation, Accuracy

ABSTRACT:

The verification of a measurement system is an essential part of system development. For this purpose, various guidelines can be used to evaluate and validate photogrammetric systems. However, these guidelines are only designed to validate systems that observe a static scene. Hence, these guidelines cannot validate measurement systems that observe dynamic scenes. In addition, reference data is not available for most systems, making verification significantly more difficult or not a practical solution. In this work, a simulation-based verification approach is presented. The presented approach allows the analysis of complex systems and the investigation of specific processing steps. The approach is based on a Monte Carlo simulation, which only requires the probability density distributions of the input data and synthetic reference data. For this purpose, the probability density distributions of the input data are determined by kernel density estimation to generate realistic input data. The application is a wind tunnel test, where aerodynamic and structural dynamic phenomena are observed at a wind turbine model. The measurement system consists of four high-speed cameras, which acquire the rotor blades' deformations. The objective of the simulation is to evaluate the complete process regarding the accuracy and precision of the measurement system. Experimental data can be used to estimate the quality of the simulation. It was shown that the simulation produces realistic results and that it is suitable for validating dynamic measurement systems. The simulation showed that the precision and accuracy of the system are highly dependent from the estimation of the self-motion. The achieved accuracy is still high and allows the detection of small-scale blade deformations.

1. INTRODUCTION

The achievable accuracy of photogrammetric measurement systems is subject to several impact factors. Therefore, external and internal influences must be considered by the system development. External factors, like temperature and air pressure changes, modify the measurement system's stability. These instabilities can decrease the quality of the interior and exterior orientation. In addition, internal factors, based on the used algorithms, camera, lenses, and configuration, can modify the quality of image measurements and derivate information. Estimating the influences and verifying accuracy and precision is not trivial. Especially for industrial and medical applications, where the highest accuracy and precision are necessary, it is an essential task in developing photogrammetric systems.

For this purpose, highly accurate reference artefacts are acquired and evaluated based on a defined procedure, which provides information about the influence of environmental influences, hardware, and software. For this reason, different approaches for verification have been developed in recent decades and standardized in the form of guidelines (GUM, VDI). For close-range photogrammetric systems, the German guideline VDI 2634 can be used to verify area-based (Finke and Bartelt, 2010) and point-based systems (Hastedt et al. 2018). Furthermore, comparing different systems is possible (Kalinowski et al. 2022). However, not every system can be evaluated with the same quality. For example, a homogenous texture of the artefacts can lead to incorrect correspondences if the method used is based on heterogeneous gradients. Therefore, some authors use artefacts that are different from the guideline, e.g., textured dumbbell bars or naturally textured objects, for the investigation of matching algorithms (Nietiedt et al., 2020) or commercial systems (Kersten et al., 2018). Furthermore, the VDI guideline is only defined for the acquisition of static scenes. The guideline cannot verify photogrammetric systems that acquire dynamic scenes.

Due to the experimental characteristics, accuracy validation of a dynamic system is not a trivial task. For example, using a highly accurate artefact that exhibits reproducible dynamics is possible in principle but not practical in all applications. Raguse uses a rotating test field to verify a measurement system in the field of car safety tests (Raguse, 2008). Other authors use instead reference data regarding the occurring kinematic properties of the object (Blume et al. 2010, Afrouz et al. 2019). The reference data are determined with accelerometers and gyroscopes and form the basis for comparing the photogrammetric data. These approaches are time-consuming and not applicable in all experimental environments, which makes it necessary to use simulations based on purely synthetic or very small datasets.

Simulation-based accuracy investigations are used in many disciplines when the measurement system is too complex for classical error propagation or only small data samples are available. For this purpose, different statistical methods can be used. These methods simulate the process or the measurement system based on given samples or probability density functions (pdf) and generate new results samples. From the calculated result samples, the mean values of the parameters and the statistic can be derived.

One of these simulation methods is the bootstrap method, which does not require information about the probability density function of the input parameters (Bishop, 2006). Instead, new subsamples are generated based on the existing samples based on the empirical probability distribution. Therefore, the method is based on the principle of resampling and requires only a small sample to obtain the desired statistical parameters. For example, Lösler et al. (2018) use this method for shape analysis of a VLBI

telescope, where the confidence intervals are finally determined by kernel density estimation. A popular simulation method is the Monte Carlo simulation (MCS), which is based on the principle of large numbers. The MCS aims to numerically simulate complex processes for which the probability distributions of the input parameters are required. The MCS finds application for the accuracy investigation of a Lidar system, which is used for the determination of pitch angles of rotor blades of a wind turbine (Helmig et al., 2020). Other authors apply the method to investigate bundle adjustments (Hastedt, 2004) and to analyze the 6DoF determination (Luhmann, 2009).
A disadvantage of MCS is the long computation times due to the high number of simulation runs. Furthermore, the probability density function of the input parameters must be known. Nevertheless, MCS is a very flexible method, which allows the consideration of different impact factors. Since no real data has to be available, the method is interesting for the uncertainty analysis of measurement systems that observe a dynamic scene.

In this publication, an MCS for the accuracy investigation of a high dynamic photogrammetric measurement system is presented and compared with experimental investigations. Furthermore, the method of kernel density estimation is explained in order to determine realistic probability density functions of the input parameters for the MCS. For this purpose, the method of MCS and kernel density estimation are explained in more detail.

2. METHOD

2.1 Monte Carlo simulation

The Monte Carlo simulation is used to analyze the dynamic measurement system. The basis of the simulation is the functional model, the probability density functions of the input parameters, and the number of simulation runs. The procedure is shown schematically in Figure 1.

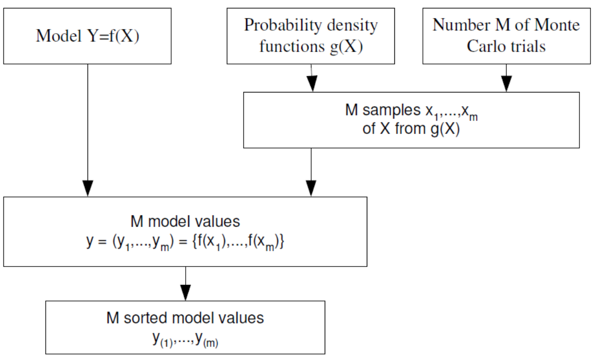

Figure 1. Workflow of the Monte Carlo simulation (Cox et al., 2001).

The model represents the measurement system to be simulated. The required input parameters (observations and model parameters) are generated using the respective probability density functions for each simulation run. The measurement system's results (usually 3D coordinates) can be determined by equation 1, and the accuracy can be estimated by equation 2. Alternatively, if error-free reference data are available, the RMS of the deviations from the reference data can be calculated. (Luhmann et al., 2019)

$$\hat{y} = \frac{1}{n}\sum_{i=1}^{n} y_i \tag{1}$$

$$\Sigma_{\hat{y}} = \frac{1}{n-1}\sum_{i=1}^{n}((y_i - \hat{y})(y_i - \hat{y})^T \tag{2}$$

2.2 Kernel density estimation

Essential for executing the MCS is the availability of the probability density functions of the input data. These can be approximated by kernel density estimation if several input data samples are available. Kernel density estimation (equation 3) is a nonparametric statistical procedure approximating the local density function at each sample point x. By cumulating all kernel functions $K(x)$ of the sample, the global density function $f(x)$ can be approximated (Bishop, 2006).

$$f(x) = \frac{1}{nh}\sum_{i=1}^{n} K\left(\frac{x - x_i}{h}\right) \tag{3}$$

Any function that satisfies equations 4 and 5 can be used as a kernel function.

$$K(u) \geq 0 \tag{4}$$

$$\int K(u)\, du = 1 \tag{5}$$

A typical kernel function is a Gaussian function (eq. 6) that leads to equation 7 when used in equation 3.

$$K(x) = \frac{1}{\sqrt{2\pi}} exp\left(-\frac{1}{2}x^2\right) \tag{6}$$

$$f(x) = \frac{1}{n}\sum_{i=1}^{n} \frac{1}{\sqrt{2\pi h^2}} exp\left(-\frac{\|x - x_i\|^2}{2h^2}\right) \tag{7}$$

The result of the approximation depends on the choice of the bandwidth h. The bandwidth can be estimated for univariate Gaussian distributions according to equation 8 (Silverman, 1986).

$$h_{opt} = \left(\frac{4}{3}\right)^{\frac{1}{5}} \sigma n^{-\frac{1}{5}} \tag{8}$$

The influences of different bandwidths are shown in Figure 2. Here, the real but unknown probability density function is a Gaussian distribution (red) approximated with different scales of the sigma. If the bandwidth is small (yellow), local maxima are modeled. On the contrary, a smoothness effect can be seen if the approximate bandwidth is too big (green). The approximation with equation 8 (purple) also fits not perfectly due to the small number of samples.

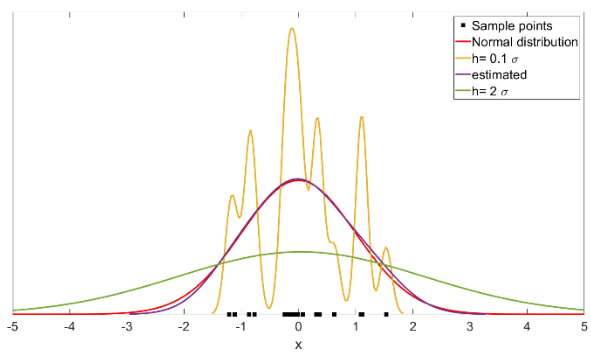

Figure 2. Influence of different bandwidths on probability density function.

3. APPLICATION

The application for simulation-based accuracy investigation is given by wind tunnel experiments for the investigation of fluid-structure interactions (FSI) (Nietiedt et al., 2022). This phenomenon describes the interaction of a flexible structure with the surrounding wind flow. The interaction is a complex phenomenon that can be observed in various applications. FSI is especially interesting in wind energy science, as it can lead to additional loads on the structure and thus to shorter lifetimes of wind turbines (Hansen et al., 2006). The experiments aim to reproduce the fluid-structure interaction in the wind tunnel and to observe this phenomenon on a rotating wind turbine model. The obtained data can be used to validate CFD simulations or help to understand the phenomenon better.

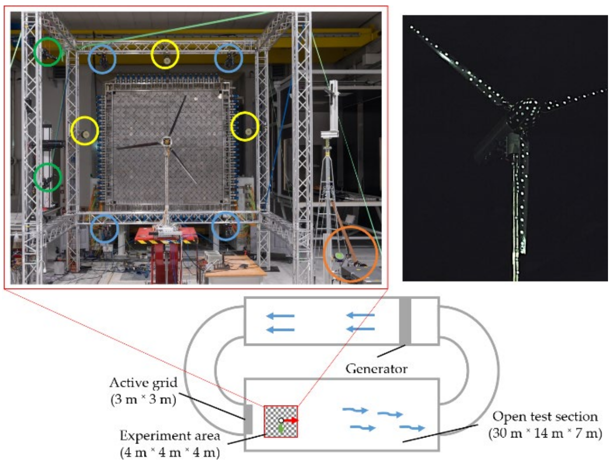

Figure 3. Measurement setup in the wind tunnel with the active grid in the background. The green and red arrow define the global coordinate system. The blue arrows show the wind flow direction. On the right side, the MoWiTO with measurement targets.

The used wind turbine MoWiTO 1.8 is a model of a real turbine and can be seen in Figure 3. The turbine has a blade length of 900 mm and a rotational speed of 50 m/s at the tip position. Compared to the reference wind turbine, the geometric scale is 1:70, and the time scaling factor is 50:1. Each blade weights 82 grams and is constructed with carbon fiber. For the analysis of the FSI, data about the aerodynamic and structural dynamic behavior of the turbine are needed. For this purpose, several experiments were realized in the wind tunnel of the University of Oldenburg. The wind tunnel is built in the Göttingen design and has an open test section of 30 m x 14 m. 4 generators can produce wind speeds of up to 32 m/s (open test section). An active grid is used to modify the laminar wind flow. The active grid is located in front of the outlet of the wind tunnel and has a size of 3 m x 3 m. The grid consists of 80 shafts with numerous diamond-shaped flaps. Every shaft can be controlled individually. This allows to generate real wind situations in a reliable and repeatable manner.

The measurement setup consists of two synchronized measurement systems. A commercial PIV system (2D-3C) is used to acquire the wind flow. The PIV system consists of two high-speed cameras (green) and a powerful laser (orange). A photogrammetric measurement system (blue) was developed to acquire the structural behavior. A global coordinate system is defined to combine the acquired wind flow and deformation by a common coordinate system. Here, the X-axis (red arrow Figure 3) is aligned to the wind direction and the Z-axis to the ground. The origin of the coordinate system is aligned with the rotation center of the turbine. The coordinate system is realized with targets on the nacelle.

3.1 Photogrammetric measurement system

The photogrammetric measurement system consists of four high-speed cameras. Due to the high rotation speed, only exposure times of max. 50 µs can be used. In order to illuminate the measurement field (2 m x 2 m) sufficiently, four LED lamps (yellow) are used. The properties of the measurement system are summarized in Table 1.

Camera	3x PCO dimax Hd+ 1x PCO dimax S4
Lens	35 mm Zeiss
Distance to object	3.5 m
Baseline	3 m
GSD	1 mm
Frame rate	600 Hz

Table 1. Properties of the photogrammetric system.

The workflow of the measurement system is shown in Figure 4. Before each experiment starts, the measurement system is calibrated by a test field calibration. After acquiring the image sequences, forward intersections compute the object coordinates of the model (see Figure 3 right). These object coordinates cannot be directly interpreted as point sequences because the matching of the uncoded object coordinates fails due to ambiguities and the self-motions of the turbine. Therefore, a Kalman filter is used to determine the self-motions of the turbine (self-rotation and tower vibration). The Kalman filter determines and predicts the self-motions based on the static reference epoch and the measurement targets on the nacelle of the respective epochs. Based on the predicted self-motion, the points on the blades can be successively matched to the point trajectories by a nearest-neighbor analysis. The determined self-motions can be eliminated by transforming the object coordinates. The corrected object coordinates form the basis for deformation analysis. The desired deformations result from the difference to the static state of the turbine, whereby the deformation only exists in the wind direction. The deformations of the rotor blades are primarily dependent on the respective wind situation and are up to 34 mm.

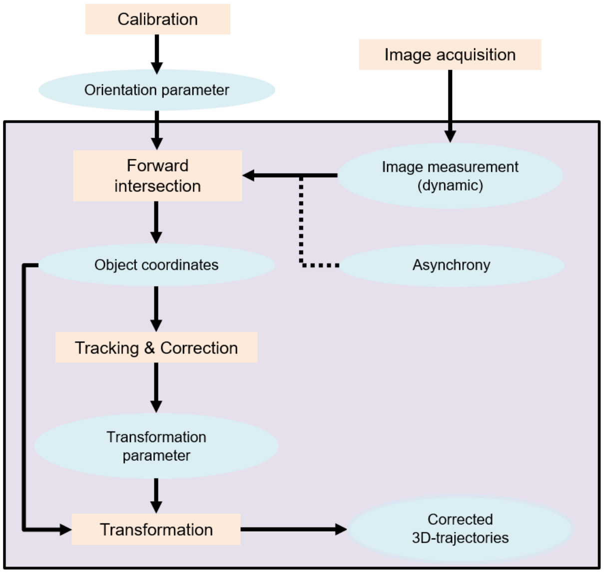

Figure 4. Workflow of the photogrammetric measurement system.

3.2 Accuracy investigation

The accuracy investigation of the photogrammetric measurement system is examined by simulation and experimental verification. The analysis aims to estimate the precision and accuracy of the system.

Here, the precision describes the quality of the deformation behavior and not the standard deviation of the determined object coordinates. Effects, which influence the absolute position, are not taken into account. In contrast, information about the accuracy includes these effects, which can influence the fusion with the aerodynamic information.

3.2.1 Experimental

For the experimental verification, the wind turbine is not affected by wind loads and is rotated manually at 20° per each step. In total, 18 positions can be used for the shape analysis, whereby only the object coordinates on the tip position are considered. The blade movements correspond to a circular trajectory, which can be determined by a best-fit circle. The determined residuals of the individual object coordinates are used as a parameter for the precision. However, only the quality of the forward intersection will be verified. The influence of the tracking and elimination step cannot be investigated experimentally. Therefore, the experiments are only used for the verification of the simulation.

3.2.2 Simulation

The accuracy estimation cannot be done using shape analysis because independent reference data are not available. Instead, the accuracy is determined using MCS. Furthermore, the simulation is applied to estimate the precision of the whole workflow.

In the scope of the simulation, the essential components of the photogrammetric system are investigated, represented by the purple area in Figure 4. Only the calibration is considered as given. The interior and exterior orientation parameters and the image measurements of the dynamic object coordinates are used as input data. In principle, extension by asynchronies is possible. However, this was not realized for this application because asynchronies between the cameras and PIV system are not relevant in this work. The required pdfs are partly based on assumptions. Gaussian distributions are assumed for the parameters of the interior and exterior orientation. The respective standard deviations, based on the statistics of the bundle adjustment, can be taken from Table 2.

Parameter	Standard deviation
Interior orientation	
Principal distance	0.0015 mm
Principal point x‘	0.0027 mm
Principal point y‘	0.0024 mm
A1	6.2859e-007
A2	9.3301e-009
A3	4.1278e-011
B1	5.5563e-007
B2	5.1767e-007
C1	7.5391e-006
C2	7.9484e-006
Exterior orientation	
X	0.102 mm
Y	0.124 mm
Z	0.270 mm
Rotation X (ω)	0.000090°
Rotation Y (φ)	0.000065°
Rotation Z (κ)	0.000099°

Table 2. Standard deviation of interior and exterior orientation.

The determination of the pdfs from the image measurements of the (dynamic) object points is done using kernel density estimation, whose density functions are shown in Figure 5. The functions closely approximate a Gaussian distribution. However, the empirically determined standard deviation is larger by a factor of 2 than the standard deviations from the image measurement (best-fit ellipse).

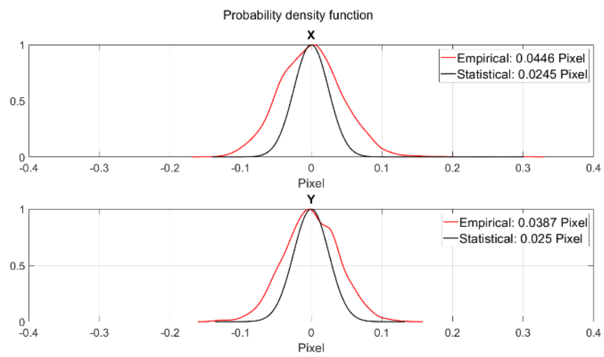

Figure 5. Figure placement and numbering.

The simulation consists of 10,000 runs, where the whole process is simulated. The size of a data set is 78 epochs, which is equivalent to one complete rotation of the turbine.

4. RESULTS

The results of the validation can be split into three sections. In the first section, the quality of the simulation is determined based on the experimental shape analysis. Furthermore, the influence of the kernel density estimation is determined. For this purpose, the simulation is performed with assumption-based probability density functions and with the results of the kernel density estimation and compared with the experimental results. The second and third sections describe the precision and accuracy investigations made by simulation.

4.1 Verification of the simulation

Table 3 summarizes the comparison of the shape analysis via experiment and simulation. Here, *Sim_sto* means that the probability density distributions for the image measurements are assumed to have a Gaussian distribution with the standard deviation of the image measurement. *Sim_kde* refers to the resulting pdfs when kernel density estimation is used.

	Experimental	*Sim_sto*	*Sim_kde*
RMS	0.08 mm	0.03 mm	0.05 mm

Table 3. Results of the shape analysis after the forward intersection.

The experimental verification shows that the detection of the deformation behavior is performed with high accuracy. The achievable RMS is 0.08 mm, thus allowing the determination of object coordinates with high quality. The discrepancy between the experimental investigation and the simulations is quite impressive. For example, the achievable RMS is smaller by almost a factor of 3 for stochastic input data and is, therefore, clearly estimated too optimistically. A comparison with *Sim_kde* also shows a difference of a factor of 1.5. The difference can probably be explained by the fact that not all data were determined using kernel density estimation. Since *Sim_kde* approximates better by a factor of 2 than *Sim_sto*, it can be expected that the kernel density estimation can lead to an improved simulation.

4.2 Precision

The shape analysis to estimate the precision of the measurement system is performed for several radial positions on the blades, which are illustrated in Figure 6.

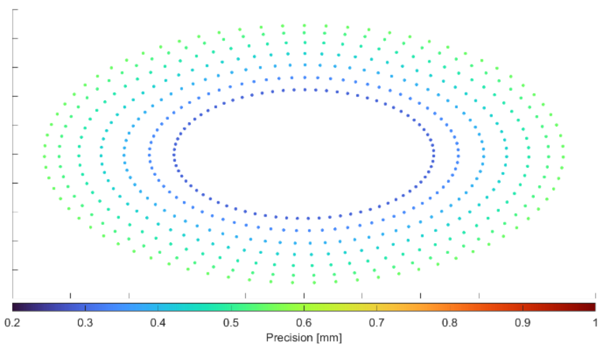

Figure 6. Precision of the photogrammetric measurement system.

The simulation-based determination of the precision for the whole workflow shows an average RMS of 0.42 mm. However, the precision is not homogenous, and a radial systematic can be observed. The highest precision can be reached at the root of blades with 0.29 mm. The lowest precision is at the tip position with 0.54 mm, which differs significantly from the experimental verification. A reason for the occurrence is probably the determination of the self-motion, which is obtained after the forward intersection. However, an investigation of the accuracy is necessary to estimate the impact of self-motion.

4.3 Accuracy

The photogrammetric measurement system's accuracy after determining the object coordinates is shown in Figure 7. Here, each point visualizes a measurement position, and the color visualizes the RMS value. The achievable accuracy level is spatially homogeneous and shows an average RMS of 0.39 mm.

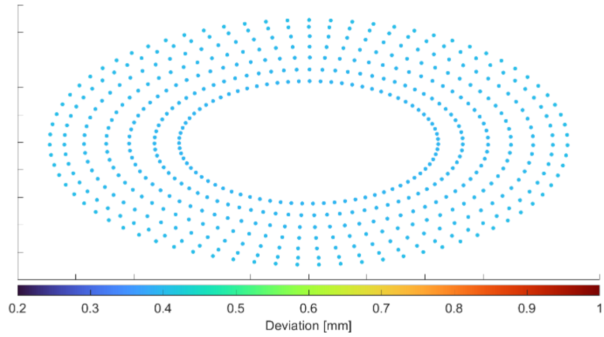

Figure 7. Accuracy of the different measurement positions after the forward intersection.

Figure 8 shows the deviation of the self-motion to the reference data set. It should be noted that the deviations of the rotations are shown as a metric deviation of the tip position for a uniform representation. Here, a drift effect can be seen for all parameters due to the sequential determination of the rigid body movements. In addition, only a maximum of 22 points can be observed on the nacelle, which can be used for utilizing a Kalman filter. Furthermore, the points are located near the center of rotation, which means that even the smallest uncertainties of the rotation angles can lead to large deviations at the blade tip due to leverage effects. The deviations are up to 0.5 mm for the translations and 1 mm for the rotations.

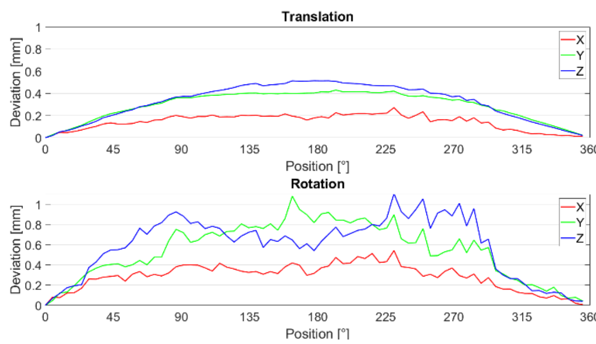

Figure 8. Accuracy of the self-motion. The rotations are shown as metric deviations.

Figure 9 shows the spatial accuracy level after the entire processing. Here, clear systematics can be seen due to the previous process step, leading to an increased average RMS of 0.51 mm. The systematic increase the RMS values with increasing radius, like the precision values. The maximum RMS is up to 0.86 mm at the tip position. Nevertheless, the measurement system achieves in all positions sub-pixel accuracy and satisfies the expectations.

https://doi.org/10.5194/isprs-archives-XLVIII-2-W2-2022-95-2022

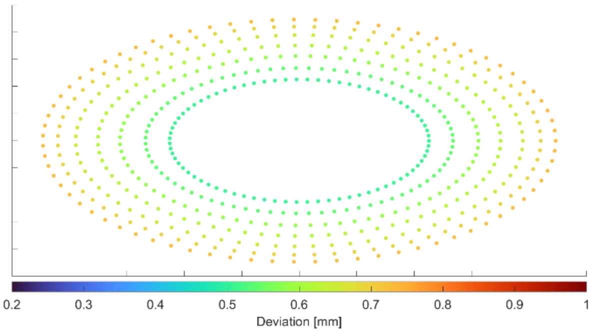

Figure 9. Accuracy of the different measurement positions after the complete processing.

5. CONCLUSION

Accuracy specifications for photogrammetric measurement systems are usually made by error propagation or using different guidelines. However, these cannot be transferred to systems that observe dynamic scenes or have complex processing structures. In order to obtain accuracy information for this type of measurement system, complex and time-consuming experiments are necessary. However, experimental verifications cannot be realized in all environments. Thus, simulations must be applied. Simulations are a practical alternative, but the method and realization of the simulation are essential for the quality of the obtained results. A widely used method is the Monte Carlo simulation. Here, only input data and the algorithms of the respective measurement system are required. Disadvantages of the simulation are that the probability density functions for generating the input data must be known, and long computing times are required.

A verification approach for a dynamic measurement system is presented based on a Monte Carlo simulation. The required probability density functions of the input data are not based on assumptions. Instead, they are approximated by the kernel density estimation method.

The application is a measurement system for acquiring aerodynamic and structural dynamic phenomena on rotating wind turbine models. The procedures are performed in a wind tunnel to provide reproducible and realistic environmental conditions. Due to the high dynamics and the high processing complexity, validation by using error propagation is not possible. Also, experimental approaches are only possible with high effort. Furthermore, experimental validation cannot evaluate all processing components in more detail. Nevertheless, practical investigations could be realized, which are used to verify the simulation.

It was shown that the kernel density estimation achieves significantly more realistic results. While the difference to the experimental results is a factor of 3 when using assumption-based distribution functions, the kernel density estimation performs better by a factor of 2. The remaining discrepancy can probably be explained by the fact that not all input data were determined by kernel density estimation. Nevertheless, the potential of Monte Carlo simulation and kernel density estimation could be demonstrated.

For the analysis of the application, it was shown that precision and accuracy highly depend on the tracking algorithm used. For example, the precision is 0.05 mm before the elimination of the self-motion. After the elimination, the average is 0.42 mm instead. A similar characteristic can also be observed in the accuracy of the measurement system. Here, the average accuracy increases from 0.39 mm to 0.51 mm. This effect can be attributed to the determination of self-motion. Unfortunately, only targets on the nacelle of the system can be used. Even the smallest deviations of the rotations lead to large deviations at the blade tip due to leverage effects. Due to the experimental setup, an improved acquisition of the self-motions is almost not possible. Only the use of further information about self-motion can improve the determination. Therefore, the next development steps aim to integrate kinematic information (e.g., rotational speed) into the process. It is assumed that the integration can improve the measurement system's precision and accuracy.

ACKNOWLEDGEMENTS

This work was funded by the Deutsche Forschungsgemeinschaft (DFG, German Research Foundation) - project number 497532406.

REFERENCES

The Association of German Engineers, 2012. VDI-Standard: VDI/VDE 2634 Optical 3-D measuring systems - Optical systems based on area scanning. Beuth Verlag.

Joint Committee for Guides in Metrology, 2008. Evaluation of Measurement Data—Guide to the Expression of Uncertainty in Measurement. International Bureau of Weights and Measures (BIPM).

Afrouz, S. G., Razavi, M. R., Pourkand, A., Wilson, C. M. D., 2019. Dynamic Displacement of an Aluminum Frame Using Close Range Photogrammetry. *Buildings*, 9(176). doi:10.3390/buildings9080176.

Bishop, M. C., 2006: *Pattern Recognition and Machine Learning*. Springer. New York, USA. 738 p.

Blume, K., Röger, M., Schlichting, T., Macke, A., Pitz-Paal, R., Dynamic photogrammetry applied to a real scale heliostat: Insights into the wind-induced behaviour and effects on the optical performance. *Solar Energy*, 212, 297-308, https://doi.org/10.1016/j.solener.2020.10.056.

Cox, M. G., Dainton, M. P., Harris, P. M., 2001: Software Specifications for Uncertainty Calculation and Associated Statistical Analysis; NPL Report CMSC 10/01.

Finke, T., Bartelt, A., 2010. Anwendung der Richtlinie VDI/VDE 2634 Blatt 3 - ein Erfahrungsbericht. In Luhmann/Schumacher (eds.): Photogrammetrie, Laserscanning, Optische 3D-Messtechnik – Beiträge der 9. Oldenburger 3D-Tage, 80-87.

Hansen, M.O.L., Sørensen, J.N., Voutsinas, S., Sørensen, N., Madsen, H.A., 2006. State of the art in wind turbine aerodynamics and aeroelasticity. *Prog. Aerosp. Sci.* 42, 285–330.

Hastedt, H. 2004. Monte-Carlo-Simulation in close-range photogrammetry. *The international archives of the photogrammetry, remote sensing and spatial information sciences*, 35, 18 - 23.

Hastedt, H., Rofallski, R., Luhmann, T., Rosenbauer, R., Ochsner, D., Rieke-Zapp, D. (2018): Prototypic development and evaluation of a medium format metric camera. *The International Archives of the Photogrammetry, Remote Sensing and Spatial*

Information Sciences, Volume XLII-2, 2018, 441-448, doi: 10.5194/isprs-archives-XLII-2-441-2018.

Helmig, P., Poeck, N., v. Freyberg, A., Sorg, M., Fischer, A., 2022. Dynamic optical deformation measurements on wind turbines. *Journal of Physics: Conference Series*, 2265 (2022), doi:10.1088/1742-6596/2265/2/022100.

Kalinowski, P., Hindmarch, J., Luhmann, T., 2022. Accuracy investigations of hand-held scanning system using different dumbbell artefacts. *Int. Arch. Photogramm. Remote Sens. Spatial Inf. Sci*., XLIII-B2-2022, 401–407, doi: 10.5194/isprs-archives-XLIII-B2-2022-401-2022.

Kersten, T. P., Lindstaedt, M., Starosta, D., 2018. Comparative geometrical accuracy investigations of hand-held 3D scanning systems – an update. *Int. Arch. Photogramm. Remote Sens. Spatial Inf. Sci.* XLII-2, 487–494. doi.org/10.5194/isprs-archives-XLII-2-487-2018.

Lösler, M., Eschelbach, C., Hass, R., 2018. Bestimmung von Messunsicherheiten mittels Bootstrapping in der Formanalyse. *Zeitschrift für Geodäsie, Geoinformation und Landmanagement*, 4,224-232.

Luhmann, T. 2009. Precision potential of photogrammetric 6DOF pose estimation with a single camera, *ISPRS Journal of Photogrammetry and Remote Sensing*, Volume 64, Issue 3, 275-284, https://doi.org/10.1016/j.isprsjprs.2009.01.002.

Luhmann, T., Robson, S., Kyle, S., Boehm, J., 2019: *Close-Range Photogrammetry and 3D Imaging*. 3rd ed., Walter de Gruyter, Berlin, 822 p.

Nietiedt, S., Kalinowski, P., Hastedt, H., Luhmann, T., 2020. Accuracy Investigations of Image Matching Techniques by Means of a Textured Dumbbell Artefact. *Int. Arch. Photogramm. Remote Sens. Spatial Inf. Sci*., XLIII-B2-2020, 791–796, doi: 10.5194/isprs-archives-XLIII-B2-2020-791-2020.

Nietiedt, S., Wester, T. T.B., Langidis, A., Kröger, L., Rofallski, R., Göring, M., Kühn, M., Gülker, G., and Luhmann, T., 2022. A Wind Tunnel Setup for Fluid-Structure Interaction Measurements Using Optical Methods. *Sensors*, 22(13). https://doi.org/10.3390/s22135014.

Raguse, K. 2007: Dreidimensionale photogrammetrische Auswertung asynchron aufgenommener Bildsequenzen mittels Punktverfolgungsverfahren. *Fakultät für Bauingenieurwesen und Geodäsie- Dissertation*, Hannover.

Silverman, B. W., 1986: *Density Estimation for Statistics and Data Analysis*. Monographs on Statistics and Apllied, Vol. 26, Chapman and Hall, London.